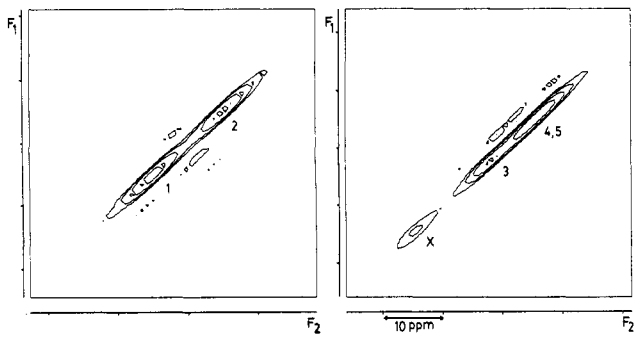

Figure 3. Contour plot of a 2D exchange spectrum (mixing time τ_m = 40 ms) of a nonspinning rubber sample with high-power proton decoupling during the evolution and the detection period. For the assignment of the lines, see Figure 1. The line denoted X is from the antidegradant. The fact that the lines are drawn out along the diagonal shows that they are inhomogeneously broadened.

result may point to the absence of diffusion on a time scale of 40 ms, in which case the relatively small interchain dipolar interactions must be due to a large distance between different segments. An alternative explanation can be, however, that reorientations are limited to small regions, i.e., in voids between filler particles, where the magnetic field is rather constant. This point will be investigated further.

Conclusions

From the above-mentioned experiments it can be concluded that the effect of the carbon black filler particles on the ^{13}C NMR line width of the rubber is twofold. First, the filler particles introduce microscopic inhomogeneities by susceptibility effects. Second, the filler does not allow the chains to move in a random way, so residual dipolar couplings are present. Such anisotropy, however, is also caused by the presence of chain entanglements. Both effects can be averaged to a great extent by MAS, allowing J resolved spectra to be recorded in the solid state. By comparison to adamantane the interchain dipolar interaction is surprisingly small. A 2D exchange experiment, however, cannot detect molecular diffusion on a time scale of ~40 ms.

Acknowledgment. We thank J. van Os for his technical assistance and Prof. Dr. E. de Boer for critically reading the manuscript. This work was carried out under the auspices of the Netherlands Foundation of Chemical Research (SON) and with the aid of the Netherlands Organization for the Advancement of Pure Research (ZWO).

Registry No. Adamantane, 281-23-2.

References and Notes

(1) (a) Terao, T.; Miura, H.; Saika, A. *J. Chem. Phys.* **1981**, *75*, 1573. (b) Terao, T.; Miura, H.; Saika, A. *J. Magn. Reson.* **1982**, *49*, 365. (c) Terao, T.; Miura, H.; Saika, A *J. Am. Chem. Soc.* **1982**, *104*, 5228. (d) Miura, H.; Terao, T.; Saika, A. *J. Magn. Reson.* **1986**, *68*, 593.
(2) (a) Zilm, K. W.; Grant, D. M. *J. Magn. Reson.* **1982**, *48*, 524. (b) Mayne, C. L.; Pugmire, R. J.; Grant, D. M. *J. Magn. Reson.* **1984**, *56*, 151.
(3) Haeberlen, U. *Adv. Magn. Reson.* **1976**, Supplement I.
(4) Maricq, M. M.; Waugh, J. S. *J. Chem. Phys.* **1979**, *70*, 3300.
(5) (a) Gutowsky, H. S.; Meyer, L. H. *J. Chem. Phys.* **1953**, *21*, 2122. (b) Gutowsky, H. S.; Saika, A.; Takeda, M.; Woessner, D. E. *J. Chem. Phys.* **1957**, *27*, 534.
(6) Duch, M. W.; Grant, D. M. *Macromolecules* **1970**, *3*, 165.
(7) Bax, A. *Two-Dimensional Nuclear Magnetic Resonance in Liquids*: D. Reidel: Dordrecht, 1982.
(8) Resing, H. A. *Mol. Cryst. Liq. Cryst.* **1969**, *9*, 101.
(9) McCall, D. W.; Douglass, D. C. *J. Chem. Phys.* **1960**, *33*, 777.
(10) Smith, G. W. *J. Chem. Phys.* **1961**, 35, 1134.
(11) Schaefer, J. *Macromolecules* **1972**, *5*, 427.
(12) Schaefer, J.; Chin, S. H.; Weissman, S. I. *Macromolecules* **1972**, *5*, 798.
(13) Dybowski, C. R.; Vaughan, R. W. *Macromolecules* **1975**, *8*, 50.
(14) (a) English, A. D.; Dybowski, C. R. *Macromolecules* **1984**, *17*, 446. (b) English, A. D. *Macromolecules* **1985**, *18*, 178.
(15) (a) Cohen-Addad, J. P. *J. Chem. Phys.* **1974**, *60*, 2440. (b) Cohen-Addad, J. P.; Faure, J. P. *J. Chem. Phys.* **1974**, *61*, 1571. (c) Cohen-Addad, J. P. *J. Phys.* (*Les Ulis, Fr.*) **1982**, *43*, 1509. (d) Cohen-Addad, J. P.; Dupeyre, R. *Macromolecules* **1985**, *18*, 1612.
(16) Garroway, A. N.; VanderHart, D. L.; Earl, W. L. *Philos. Trans. R. Soc. London, A* **1981**, *299*, 609.
(17) Stejskal, E. O.; Schaefer, J.; Waugh, J. S. *J. Magn. Reson.* **1977**, *28*, 105.
(18) Andrew, E. R. *Philos. Trans. R. Soc. London A* **1981**, *299*, 505.
(19) Jeener, J.; Meier, B. H.; Bachmann, P.; Ernst, R. R. *J. Chem. Phys.* **1979**, *71*, 4546.
(20) Szeverenyi, N. M.; Sullivan, M. J.; Maciel, G. E. *J. Magn. Reson.* **1982**, *47*, 462.
(21) Burum, D. P.; Linder, M.; Ernst, R. R. *J. Magn. Reson.* **1981**, *44*, 173.

Interpretation of ^{13}C NMR Sequence Distribution for Ethylene–Propylene Copolymers Made with Heterogeneous Catalysts

C. Cozewith

Exxon Chemical Company, Linden, New Jersey 07036. *Received September 29, 1986*

ABSTRACT: The utility of ^{13}C NMR diad and triad distribution data for characterizing heterogeneous Ziegler catalysts used to make ethylene–propylene copolymers is examined. Appropriate statistical criteria are established for determining whether single- or multiple-site models best fit measured sequence distributions. Least-squares data correlations for copolymers made with a variety of heterogeneous titanium catalysts indicate the copolymers are typified by broad compositional distributions and multiple catalyst species. However, a simple two-site model is adequate in some cases. The r_1r_2 of the individual sites is estimated to lie in the range 0.5 to 3.0. The average $\overline{r_1r_2}$ for heterogeneous titanium catalysts determined from polymer composition/monomer concentration data and the copolymerization equation is much lower than the value calculated from the diad distribution. Consequently this former $\overline{r_1r_2}$ does not correctly indicate copolymer sequence distribution.

Introduction

^{13}C NMR analysis for the diad and triad distribution in ethylene–propylene copolymers (EPM) is a well-established technique.[1-4] A number of authors[5-7] have attempted to obtain information on the nature of titanium-based Ziegler catalysts used for EPM synthesis by com-

0024-9297/87/2220-1237$01.50/0 © 1987 American Chemical Society

paring measured sequence distributions with the distributions expected for a first-order Markov process. From a kinetic point of view, a first-order Markov process requires that the catalyst contain only a single type of active site and the comonomer ratio at the site remain constant during chain growth. Most of the published results show that the average reactivity ratio product, $\overline{r_1r_2}$, calculated from the ethylene–ethylene (EE), propylene–propylene (PP), and ethylene–propylene (EP) diad concentrations from the equation[5]

$$\overline{r_1r_2} = 4(\mathrm{EE})(\mathrm{PP})/(\mathrm{EP})^2 \quad (1)$$

is greater than 1, and that the triad sequence distribution calculated from $\overline{r_1r_2}$ is not particularly well represented by first-order Markov statistics. Since the copolymers were synthesized at constant comonomer ratio, this result has been explained by the presence of multiple catalyst sites causing copolymer compositional heterogeneity. Cheng[8] used a more sophisticated approach to determine reactivity ratios based on a least-squares fit of spectral data to the Markov equations for diad and triad distributions. For the six polymers analyzed, Cheng reports that a first-order Markov model gave an adequate fit to the data for four polymers, while the other two were better fit by a second-order Markov (penultimate copolymerization) model. No statistical justification is stated for these conclusions.

Ross[9] derives equations for diad and triad distributions for the case of multiple catalyst species, each of which has r_1r_2 equal to 1. Analysis of data by Kakugo et al.[5] and Doi et al.[6] by this model produced a much better fit than the first-order Markov model. In a second paper[10] Ross further shows that Kakugo's data appear to be consistent with the presence of two catalyst sites, one of which polymerizes propylene poorly.

The purpose of this paper is to examine the utility of EPM ^{13}C NMR measurement of diads and triads for characterizing the number and type of active sites in the catalyst. Three models for diads and triads are considered: single catalyst species (first-order Markov), multiple catalyst species with $r_1r_2 = 1$, and two catalyst species with $r_1r_2 = 1$. A least-squares technique is described for determining model parameters, and statistical criteria are established for model suitability. It is shown that model inadequacy is related to the very broad compositional distributions that arise with certain catalysts. In addition, we find that $\overline{r_1r_2}$ derived from ^{13}C data for titanium catalysts is higher than the value obtained from fitting polymer composition/monomer concentration data to the copolymerization equation. For multiple species catalysts, r_1 and r_2 determined from the copolymerization equation do not have a direct relationship to the polymerization rate constants and do not predict sequence distribution.

Experimental Section

A. Polymerizations. Copolymerization was carried out in *n*-hexane solvent in a continuous-flow-stirred reactor at 510 kPa. Ethylene, propylene, and hexane were purified by the usual techniques to remove trace quantities of catalyst poisons. The reactor was fed by a solution of the monomers in hexane, a solution of the aluminum alkyl in hexane, and either a solution or slurry of the titanium catalyst in hexane. Flow rates were controlled by rotameters and metering pumps. The reactor was operated liquid full, and reactant concentrations were set to give a polymer concentration of 4–6 wt % in the product exiting the reactor. Solution polymerization at these conditions is free of diffusional effects. After the polymerization was quenched with water, hexane was removed from the solution by steam stripping and the polymer was dried on a hot rubber mill.

B. ^{13}C NMR Measurements. Samples were dissolved in trichlorobenzene at 4.5 wt % concentration. The ^{13}C NMR spectra were obtained at 140 °C with a pulsed Fourier transform Varian XL-400 NMR spectrometer at 100 MHz. Deuteriated *o*-dichlorobenzene was placed in a coaxial tube to maintain an internal lock signal. Instrument conditions were as follows: pulse angle, 75°; pulse delay, 25 s; acquisition time, 0.5 s; sweep width, 16 000 Hz.

The ^{13}C NMR peak area measurements were determined by spectral integration. Diad and triad concentrations were calculated from the equations presented by Kakugo et al.[5] and then normalized to give the mole fraction distribution. Polymer composition was calculated from the methine peaks,[3] the methylene peaks,[3] and the diad balance.[2] All three methods were usually in good agreement, and an average of the three values is reported for the composition.

C. Polymer Fractionation. Polymer solutions were prepared at 2% concentration in boiling *n*-hexane. Insoluble polymer was recovered as the first fraction by passing the solution through a fine mesh screen. The solution was then cooled to room temperature, and 2-propanol was added until a precipitate was observed. The precipitate was removed by filtration through a screen, and the 2-propanol addition was continued until four fractions were obtained. The remaining hexane/2-propanol solution was then evaporated to dryness to recover a final fraction. The polymers were dried in a vacuum oven for 24 h at 60 °C and then weighed and analyzed.

Model Equations

For a copolymer produced by a single catalyst species at constant comonomer concentration in the absence of diffusion or mixing effects, the monomer composition/polymer composition relationship is described by the terminal copolymerization model

$$m = M(r_1M + 1)/(r_2 + M) \quad (2)$$

where r_1 and r_2 are the reactivity ratios, m is the ratio of monomers in the copolymer, m_1/m_2, M is the ratio of monomers in the reactor, M_1/M_2, and the diad and triad concentrations follow first-order Markov statistics.

We will refer to copolymerizations having these characteristics as ideal copolymerizations.

For this model, nine equations can be derived[5,11] that relate the diad and triad concentrations to P_{12} and P_{21}, the probability of propylene adding to an ethylene-ended chain and the probability of ethylene adding to a propylene-ended chain, respectively. Thus a fit of ^{13}C NMR data to these equations yields P_{12} and P_{21} as the model parameters, from which r_1 and r_2 can be obtained from the relationships

$$r_1M = (1 - P_{12})/P_{12} \quad (3)$$

$$r_2/M = (1 - P_{21})/P_{21} \quad (4)$$

The corresponding equations for random copolymerization with $r_1r_2 = 1$ (zero-order Markov process) can also be found in ref 11. In this case eq 2 simplifies to

$$m = r_1M \quad (5)$$

and the ethylene fraction in the polymer, E, is equal to $1 - P_{12}$. This allows the diad and triad equations to be written in terms of the polymer composition

$$\mathrm{EE} = E^2 \quad (6)$$

$$\mathrm{EP} = 2E(1 - E) \quad (7)$$

$$\mathrm{PP} = (1 - E)^2 \quad (8)$$

$$\mathrm{EEE} = E^3 \quad (9)$$

$$\mathrm{EEP} = 2E^2(1 - E) \quad (10)$$

$$\mathrm{EPE} = E^2(1 - E) \quad (11)$$

$$\mathrm{PEP} = E(1 - E)^2 \quad (12)$$

$$\mathrm{PPE} = 2E(1 - E)^2 \quad (13)$$

$$PPP = (1 - E)^3 \quad (14)$$

If a polymer is produced by a catalyst that contains a multiplicity of different active sites, the average concentration of a given sequence $\bar{L}$, will be given by

$$\bar{L} = \sum_{i=1}^{n} f_i L_i \quad (15)$$

where f_i is the mole fraction of monomer polymerized by catalyst species i, L_i is the concentration of sequence L in the polymer fraction produced by catalyst species i, and n is the number of catalyst species. L_i is a function of $(P_{12})_i$ and $(P_{21})_i$ according to the appropriate set of diad and triad equations.

For the special case where $(r_1r_2)_i = 1$, eqs 6–14 apply for the individual species and we have

$$\bar{E} = \sum f_i E_i \quad (16)$$

$$\overline{EE} = \sum f_i E_i^2 = S_2 \quad (17)$$

$$\overline{EP} = 2\sum f_i E_i(1 - E_i) = 2\bar{E} - 2S_2 \quad (18)$$

$$\overline{PP} = \sum f_i(1 - E_i)^2 = 1 - 2\bar{E} + S_2 \quad (19)$$

$$\overline{EEE} = \sum f_i E_i^3 = S_3 \quad (20)$$

$$\overline{EEP} = 2\sum f_i E_i^2(1 - E_i) = 2S_2 - 2S_3 \quad (21)$$

$$\overline{EPE} = \sum f_i E_i^2(1 - E_i) = S_2 - S_3 \quad (22)$$

$$\overline{PEP} = \sum f_i E_i(1 - E_i)^2 = \bar{E} - 2S_2 + S_3 \quad (23)$$

$$\overline{PPE} = 2\sum f_i E_i(1 - E_i)^2 = 2\bar{E} - 4S_2 + 2S_3 \quad (24)$$

$$\overline{PPP} = \sum f_i(1 - E_i)^3 = 1 - 3\bar{E} + 3S_2 - S_3 \quad (25)$$

where $S_2 = \sum f_i E_i^2$ and $S_3 = \sum f_i E_i^3$ and the superscript bar denotes an average value. From the definition of S_2 and S_3 it is obvious that

$$\bar{E} > S_2 > S_3$$

These model equations are valid for any number of catalyst species as long as each has r_1r_2 equal to 1. However, the model parameters S_2 and S_3 do not yield any information about the individual catalyst species. To estimate the number of species present, eq 15 must be written explicitly for a given number of species and the resultant model tested for the quality of fit. For instance, with a two species catalyst the $\overline{PP}$ equation is

$$\overline{PP} = f_1(P_{12})_1^2 + (1 - f_1)(P_{12})_2^2$$

where the subscripts 1 and 2 refer to catalyst species 1 and 2, and the other diad and triad relationships can be derived similarly. This model has three parameters, f_1, $(P_{12})_1$, and $(P_{12})_2$. However, if we assume the polymer composition is correct, the composition relationship

$$\bar{E} = f_1(1 - (P_{12})_1) + (1 - f_1)(1 - (P_{12})_2) \quad (26)$$

allows one parameter to be expressed in terms of the other two, reducing the number of parameters to two.

With more complex models such as three species with r_1r_2 equal to 1 or two species with arbitrary r_1r_2, the number of model parameters becomes too large to determine with any statistical significance from the seven independent diad and triad data points measured in a single ^{13}C NMR spectra. Thus in this paper we limit the discussion to the three models above: single catalyst species, multiple catalyst species all with $r_1r_2 = 1$, and two catalyst species with $r_1r_2 = 1$.

For the most part, past investigators have determined model parameters from a few selected sequence measurements, for instance by use of eq 1, and then judged model applicability qualitatively by how well the model predicted the distribution of the other sequences. A superior technique,[8] used in this study, is to find the model parameters by a least-squares method that minimizes the sum of the squares of deviations between predicted and experimental values for all of the diads and triads. The confidence limits on the model parameters and the sum of the squares of deviations then provides a quantitative basis for deciding whether a particular model adequately represents the data. In this work we utilized the nonlinear least-squares program NLIN provided by the SAS Institute (Raleigh, NC) to perform the necessary calculations.

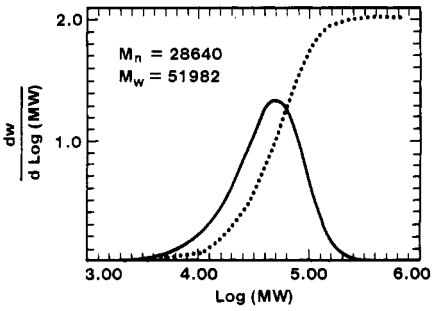

Figure 1. GPC data for ideal copolymer A.

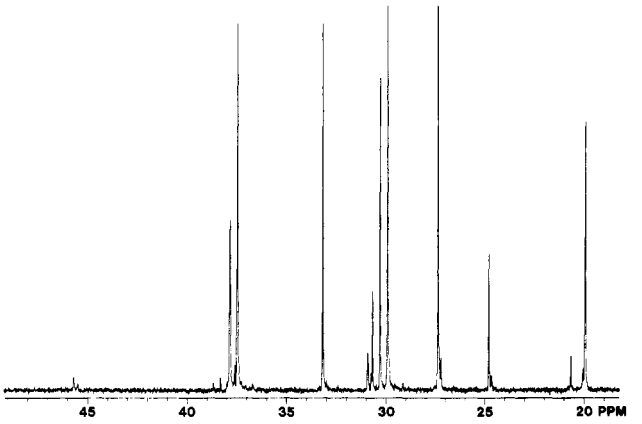

Figure 2. ^{13}C NMR spectra of ideal copolymer A.

Criteria for Model Applicability

Copolymers made by a single catalyst species in a continuous-flow-stirred tank reactor would be expected to fit the first-order Markov equations exactly. Deviations from the model would represent only experimental error. This provides a benchmark for concluding whether a particular model is acceptable. Models that give a sum of squares considerably higher than the benchmark value are most likely inappropriate. Two ideal copolymers were synthesized with a soluble titanium catalyst that yields only one active species as indicated by a unimodal, narrow MWD with $\bar{M}_w/\bar{M}_n$ equal to 1.8 (see Figure 1). This is close to the theoretically expected value of 2.0 for a single species.[12] Also, analysis of four polymer fractions obtained by 2-propanol precipitation indicated no compositional differences within experimental accuracy. The ^{13}C NMR spectra for the polymers (see Figures 2 and 3) contain no peaks due to inverted propylene addition, so simple copolymerization kinetics apply.

The measured diad and triads concentrations in Table I were fit to eq 3–11 to determine the P_{12} and P_{21} values that minimize the sum of the squared deviations. As shown by the results in Table I, there is excellent agreement between observed and calculated sequence concentrations, the sum of squares of the deviations is on the

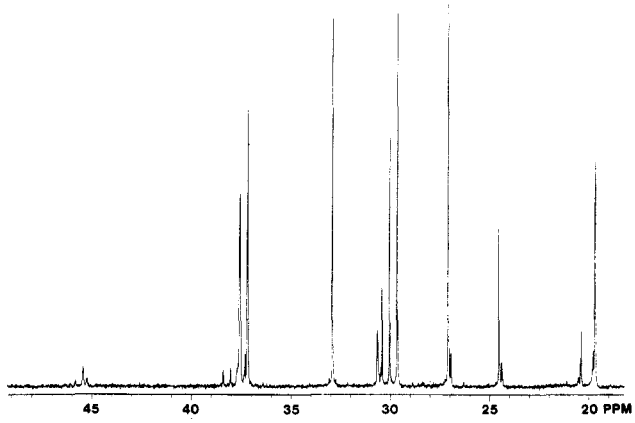

Figure 3. ^{13}C NMR spectra of ideal copolymer B.

Table I
Model Fit for Ideal Ethylene–Propylene Copolymers

	polymer A		polymer B	
	obsd	calcd	obsd	calcd
E	0.695		0.640	
EE	0.409	0.414	0.617	0.622
EP	0.554	0.556	0.318	0.327
PP	0.0369	0.0298	0.0642	0.0512
EEE	0.251	0.248	0.172	0.168
EEP	0.333	0.333	0.324	0.319
EPE	0.254	0.251	0.273	0.267
PEP	0.112	0.112	0.149	0.152
PPE	0.0503	0.0539	0.0822	0.0879
PPP	0.0	0.003	0.0	0.007
SS[a]		1.1×10^{-4}		4.4×10^{-4}
P_{21}[b]		0.903 ± 0.005		0.859 ± 0.009
P_{12}[b]		0.402 ± 0.002		0.487 ± 0.005
r_1r_2[c]		0.160		0.173

[a] SS indicates the sum of squares. [b] Standard error of estimate is indicated. [c] $r_1r_2 = (1 - P_{12})(1 - P_{21})/(P_{12}P_{21})$.

order of 10^{-4}, and the standard error of estimate for P_{12} and P_{21} is small. Furthermore, the r_1r_2 values calculated from P_{12} and P_{21} are in good agreement for the two samples, which is additional confirmation of model accuracy. For a single-species catalyst, r_1r_2 should not vary from sample to sample. From these results we conclude that the data are in accord with a first-order Markov model and the sum of the squared deviations represents for the most part the accuracy of the ^{13}C NMR analysis. This sum will obviously be different for other spectrometers run at different measurement conditions. However, we feel it is safe to assume that a sum of squares less than 10×10^{-4} is an indication that a given model adequately represents the copolymerization process. Much higher deviations would be due to a lack of fit to the model.

Analysis of EP Copolymers Made by Heterogeneous Catalysts

The single-species model was applied to the sequence data presented by Kakugo et al. for a series of EP copolymers, ranging from 13 to 75 mol % ethylene, produced by a heterogeneous $TiCl_3$ catalyst. Kakugo calculated the r_1r_2 values for each sample from the diad concentrations with eq 1 and concluded that the model was inadequate based on poor agreement between calculated and observed triad fractions. Reanalysis of this data by the least-squares technique gives the result in Table II. The sum of the squares of the deviations range from 52 to 136×10^{-4} so a lack of fit to the model is clearly indicated. The sum of the squares is about 20% higher for sequence concentrations calculated from the diad r_1r_2 value. Despite the model inadequacy, r_1r_2 is relatively constant as polymer

Table II
Analysis of the Data of Kakugo et al. by Least Squares

		$\overline{r_1r_2}$		
sample	mol % ethylene	diads	least squares	10^{-4}SS[a]
H	75	2.9	3.1	79
G	72	3.1	4.0	73
B	53	3.4	4.0	136
F	49	3.0	3.4	52
E	25	3.7	3.5	77
D	22	3.8	3.7	88
C	15	4.2	3.4	110
A	13	4.4	3.9	104

[a] Sum of the squares of the deviations.

Table III
Application of the Multiple-Species Model to the Data of Kakugo et al.

sample	mol % ethylene	$S_2 = \sum f_i E_i^2$	$S_3 = \sum f_i E_i^3$	10^{-4}SS[a]
H	75	0.605	0.515	7.9
G	72	0.570	0.487	2.7
B	53	0.354	0.281	4.6
F	49	0.307	0.230	0.77
E	25	0.112	0.0773	1.7
D	22	0.0962	0.0642	2.1
C	15	0.0538	0.0391	2.7
A	13	0.0258	0.00948	48.6

[a] Sum of the squares of the deviations.

composition varies. Note that r_1r_2 calculated from the diads trends upward as the polymer ethylene content decreases, but the sum of squares analysis indicates that no real correlation exists.

The next model to be considered is multiple species with $(r_1r_2)_i$ equal to 1. These model equations predict EEP = $2EPE$ and $PPE = 2PEP$, which provides a quick test of model applicability. The EEP/EPE and PPE/PEP ratios for the data of Kakugo et al. follow:

sample	H	G	B	F	E	D	C	A
EEP/EPE	1.55	1.78	1.56	1.88	1.75	2.00	1.50	1.40
PPE/PEP	2.00	1.86	1.82	1.91	2.10	1.80	2.43	2.00

and most of the ratios are reasonably close to 2.0 with the EEP/EPE ratio averaging 1.68 and PPE/PEP averaging 1.99. Ross's[9,10] analysis of the data of Kakugo et al. has already indicated that the results appear consistent with r_1r_2 for the individual catalyst species equal to 1. Here, we simply repeat the calculations except the appropriate constants are determined by a least-squares fit to the diad and triad equations and the sum of the squares of the deviations is used to judge model applicability.

Correlation of the data with the multiple species model (eq 39–42) gives sums of the squares less than 10×10^{-4}, except for sample A (see Table III), from which we can conclude the model fits the data very well. The confidence limits on the model parameters indicate the reduced sum of squares is indeed due to the model itself and not to the extra parameter that is introduced by going from a one- to a multiple-catalyst-species situation. We next repeat the data correlation assuming that only two species are present. As shown by the low sum of squares values in Table IV, the polymers of Kakugo et al. are unusually well described by a two-species model with $(r_1r_2)_i$ equal to 1. Differences between calculated and observed sequence concentrations, as exemplified by the results for sample B shown in the lower half of Table IV, are quite small. The composition of each of the two components, calculated from the $(P_{12})_1$ and $(P_{12})_2$ values from the correlation, indicates that one of the catalyst species polymerizes pro-

Table IV
Fit of the Data of Kakugo et al. to a Two-Species Model and Sequence Distribution for Sample B

		component 1		component 2	
sample	mol % ethylene	f_1	mol % ethylene	mol % ethylene	10^{-4}SS[A]
H	75	0.599	91.9	49.6	7.9
G	72	0.458	96.7	51.1	2.7
B	53	0.323	92.2	34.3	4.6
F	49	0.304	87.9	31.8	0.77
E	25	0.123	84.1	16.7	1.7
D	22	0.137	76.9	13.3	2.1
C	15	0.055	88.2	10.7	2.7
A	13	0.042	89.0	11.0	49

sample	PP	EP	EE	PPP	PPE	EPE	PEP	EEP	EEE
B, obsd	0.29	0.35	0.36	0.19	0.20	0.09	0.11	0.14	0.28
B, calcd	0.29	0.35	0.36	0.19	0.20	0.07	0.10	0.15	0.28

[a] Sum of the squares of the deviations.

Table V
Analysis of Ray's Data by One- and Two-Species Models and Sequence Distribution for Sample C by the Two-Species Model

		one-species model		two-species model, $(r_1r_2)_i = 1$			
sample	mol % ethylene	$\overline{r_1r_2}$	10^{-4}SS[a]	f_1	E_1	E_2	10^{-4}SS[a]
A	8.3	0.95	16				
B	14.3	1.1	9.3				
C	55.3	2.4	101	0.650	0.392	0.851	18
D	71.8	2.0	46	0.721	0.614	0.986	7
E	84.5	2.8	22	0.255	0.602	0.928	8

sample	PP	EP	EE	PPP	PPE	EPE	PPE	EEP	EEE
C, obsd	0.24	0.40	0.35	0.16	0.19	0.10	0.11	0.17	0.23
C, calcd	0.26	0.39	0.35	0.15	0.22	0.08	0.07	0.25	0.22

[a] Sum of squares of deviations

Table VI
Analysis of the Data of Doi et al. by One- and Two-Species Models

		one-species model		two-species model, $(r_1r_2)_i = 1$			
sample	mol % ethylene	$\overline{r_1r_2}$	10^{-4}SS[a]	f_1	E_1	E_2	10^{-4}SS[a]
1	70	1.88	78	0.755	0.804	0.379	20
2	60	2.08	120				
3	55	2.16	109	0.573	0.736	0.300	20
4	48	1.95	108	0.546	0.667	0.254	23
5	45	1.96	65	0.464	0.665	0.263	6

[a] Sum of the squares of the deviations.

pylene very poorly and produces a high ethylene content copolymer regardless of the propylene/ethylene monomer ratio. The amount of this component increases relative to the second component as the propylene/ethylene monomer ratio is decreased.

A similar analysis of the data of Ray et al.[2] for five ethylene–propylene copolymers made with a $TiCl_3$-based catalyst is shown in Table V. The high sums of squares for the one-species model indicate that it is not applicable. Average $\overline{r_1r_2}$ values calculated from the model parameters range from about 1 at low polymer ethylene content to 2.8 at high ethylene content. The two-species model with $(r_1r_2)_i$ equal to 1 reduces the sums of the squares appreciably and can be considered an accurate representation of the polymer for samples D and E. Sample C gives a somewhat higher sum of squares, and thus the sequence distribution is not fully explained by the model. Observed and calculated sequence concentrations for this sample are shown in the lower half of Table V. We were not able to get parameter estimates for samples A and B because the value of f_1 was so close to 1 that the nonlinear least-squares routine failed to converge. In agreement with the results in Table IV, the two-species model indicates that the polymers of Ray et al. contain a high- and a low-ethylene-content component.

We also analyzed the data of Doi et al.[6] by the same techniques. As shown in Table VI, the single-species model once again gives a large sum of squares, although $\overline{r_1r_2}$ is quite constant as polymer composition varies. A two-species model gives a better fit to the data, but it too is not completely adequate since the sums of the squares are above 10×10^{-4} except for sample 5. (Sample 2 also had a high sum of squares, but the results are not shown because of a lack of satisfactory convergence of the fitting routine.)

Table VII shows diad and triad concentrations determined by ^{13}C NMR for seven copolymers of 62–65 mol % ethylene we produced with six different Ti catalysts. All of the copolymerizations were carried out at 60–75 °C in hexane solution. Catalysts 1–4 were fed to the reactor as a slurry in hexane while catalysts 5 and 6 were fed as a hexane solution. The reactor residence time was relatively short, 10–15 min, as compared to typical reaction times with catalysts of this type.

The results in Table VIII show that neither the one-species model nor the two-species model represents the data, although the sums of the squares are less with the two-species correlation. The low values of the EEP/EPE and PPE/PEP ratios indicate that the multiple species model with $(r_1r_2)_i$ equal to 1 is not applicable either. To

Table VII
Diad and Triad Concentrations for Various Ti-Catalyzed Copolymers

			sequence analysis by ^{13}C NMR								
sample	catalyst	mol % ethylene	PP	EP	EE	PPP	PPE	EPE	PEP	EEP	EEE
1	$TiCl_3/^{1/3}AlCl_3$[a]	0.629	0.178	0.414	0.408	0.133	0.122	0.130	0.110	0.218	0.286
2	Ti/Mg/THF[b]	0.621	0.156	0.438	0.408	0.100	0.128	0.161	0.092	0.239	0.280
3	Ti-MgR_2[c]	0.651	0.133	0.440	0.427	0.060	0.138	0.172	0.091	0.245	0.294
4	Ti/Mg[d]	0.629	0.169	0.421	0.410	0.110	0.121	0.146	0.079	0.241	0.303
5	$Ti/Mg(OR)_2$[e]	0.634	0.165	0.423	0.412	0.100	0.110	0.161	0.074	0.250	0.304
6	$Ti/MgCl_2$/EHA[f]	0.649	0.156	0.369	0.474	0.100	0.089	0.181	0.067	0.219	0.345
7	$Ti/MgCl_2$/EHA[g]	0.624	0.167	0.420	0.412	0.089	0.124	0.167	0.0884	0.233	0.298

[a] Stauffer AA. $AlEt_3$ cocatalyst. [b] $TiCl_3/MgCl_2$/tetrahydrofuran complex. $AlEt_3$ cocatalyst. [c] $TiCl_4$ reduced by di *n*-hexyl magnesium. $AlEt_2Cl$ cocatalyst. [d] Ti supported on $MgCl_2$. $AlEt_3$ cocatalyst. [e] $TiCl_4$/Mg ethyl hexanoate soluble complex, Mg/Ti = 7. $Al(i\text{-}Bu)_2Cl$ cocatalyst. [f] $TiCl_4/MgCl_2$. Ethyl hexyl alcohol soluble complex, Mg/Ti = 7. $Al(i\text{-}Bu)_2Cl$ cocatalyst. [g] $AlEt_2Cl$ cocatalyst.

Table VIII
Analysis of Ti Copolymer Data by One- and Two-Species Models

		one-species model		two-species model, $(r_1r_2)_i = 1$			
sample	mol % ethylene	r_1r_2	$10^{-4}SS$[a]	f_1	E_1	E_2	$10^{-4}SS$[a]
1	62.9	1.85	126	0.200	0.252	0.723	54
2	62.1	1.30	76	0.107	0.166	0.676	29
3	65.1	1.10	43	0.279	0.448	0.718	28
4	62.9	1.61	82	0.121	0.148	0.695	19
5	63.4	1.43	89	0.071	0.019	0.681	25
6	64.9	1.81	154	0.124	0.085	0.729	52
7	62.4	1.44	87	0.152	0.217	0.697	32

[a] Sum of the square of the deviations.

Table IX
Characterization of Polymer Fractions

						one-species model	
fraction	no.	wt %	mol % ethylene	M_n[a]	M_w/M_n[a]	r_1r_2	$10^{-4}SS$[b]
hexane insol	1	32.2	83.5			2.79	44
ppt 1	2	11.2	80.0	68600	3.21	0.89	22
ppt 2	3	22.7	67.5	73780	1.99	0.51	7
ppt 3	4	19.4	51.0	44480	2.48	1.07	80
ppt 4	5	4.2	42.0			1.58	137
hexane/2-propanol sol[c]	6	10.1					

[a] By GPC. [b] Sum of the squares of the deviations. [c] Low MW grease. No analysis done.

better understand the nature of the compositional distribution leading to these results, sample 5 was fractionated by 2-propanol precipitation from hexane solution to give the six polymer fractions shown in Table IX. As can be seen from the data, the polymer compositional distribution is exceedingly broad with compositions present that range from 40 to 85 mol % ethylene. ^{13}C NMR spectra were obtained for fractions 1–5, and the one-species model correlation of the measured diad and triad concentrations produced the r_1r_2 values and the sums of the squares also given in the table. The small sum of the squares for fraction 3 indicates a narrow compositional distribution for this sample. Thus the r_1r_2 of 0.51 reflects the nature of a particular catalyst species. For the other fractions, the sum of the squares indicates a mixture of compositions is present, although the compositional distribution should be relatively narrow. As discussed later, the r_1r_2 for these fractions probably lies between the extremes of r_1r_2 for the individual catalyst species. Consequently, we can conclude that the $TiCl_4/Mg(OR)_2$ catalyst produces multiple catalyst species that range in r_1r_2 from at least 0.5 to 3.0. The high r_1r_2 associated with the highest ethylene content fraction indicates that the catalyst sites that form this fraction have a large r_1 value and polymerize propylene with difficulty. In view of this complexity, ^{13}C NMR diad and triad distribution data cannot by themselves provide much information on the nature of the catalyst. Less detailed fractionation data for the other samples in Table IX also show that the compositional distributions are quite broad.

We conclude from these results that despite the ability of the two species, $r_1r_2 = 1$ model to correlate much of the data in Table IV and V it is by no means widely applicable to all titanium-based Ziegler catalysts. Broad compositional distributions arising from multiple catalyst species can be expected for EPM made with heterogeneous catalysts, and ^{13}C NMR data must be interpreted with this in mind.

Significance of Average Reactivity Ratio Products

In view of the many authors who have applied either the diad relationship (eq 1) or composition relationship (eq 2) to calculate average reactivity ratios for catalysts that produce multiple species, it is worth considering the significance of these averages. From the equations presented by Cozewith and Ver Strate,[12] the average values of $\bar{r}_1$, $\bar{r}_2$, and $\overline{r_1r_2}$ arising from the copolymerization kinetics are given by

$$\bar{r}_1 = (\sum r_{1i}f_i/G_i)/(\sum f_i/G_i) \quad (27)$$

$$\bar{r}_2 = (\sum r_{2i}f_i/G_i)/(\sum f_i/G_i) \quad (28)$$

$$\overline{r_1r_2} = (\sum r_{1i}f_i/G_i)(\sum r_{2i}f_i/G_i)/(\sum f_i/G_i)^2 \quad (29)$$

where $G_i = r_{1i}M + 2 + r_{2i}/M$

Consequently, $\bar{r}_1$ and $\bar{r}_2$ are functions of the monomer ratio M rather than true constants, which should lead to difficulties when eq 2 is used to fit polymer composition/monomer concentration data for multiple-species catalysts. Nevertheless, all of the reported EPM studies

for a wide variety of catalysts show a good correlation with eq 2.

Calculations of average polymer compositions for two-species catalysts with assumed values for the rate constants indicate that even when $\bar{r}_1$ and $\bar{r}_2$ vary with M the relationship of polymer composition to monomer concentration can be described by eq 2 over a limited range of M. However, the r_1 and r_2 values that give the best fit to the data are empirical parameters that have no obvious connection to the copolymerization rate constants. As a result, r_1r_2 determined from polymer composition/M measurements will not correctly predict sequence distribution. This is amply demonstrated in a number of EPM studies.

From the polymer composition/monomer concentration data presented by Doi et al.,[6] we have determined

$$\bar{r}_1 = 3.42 \qquad \bar{r}_2 = 0.0924 \qquad \overline{r_1r_2} = 0.32$$

by a nonlinear least-squares fit to eq 2. The standard errors of estimate for $\bar{r}_1$ and $\bar{r}_2$ are 0.44 and 0.026. The ^{13}C NMR data for the polymers gives $\bar{r}_1$ between 6 and 10, $\bar{r}_2$ between 0.18 and 0.34 and $\overline{r_1r_2}$ equal to about 2.0, a much higher value than that obtained from the copolymerization equation. Kashiwa et al.[13] report $\overline{r_1r_2}$ equal to 0.13 for $TiCl_4/MgCl_2$/EHA–DEAC from polymer composition/monomer concentration data, while for a polymer prepared by us an $\overline{r_1r_2}$ of 1.43 was obtained by ^{13}C NMR (see Table VIII). Similarly, Kashiwa gives $\overline{r_1r_2}$ equal to 2.0 for $TiCl_4/MgCl_2$/EB–TEA, while Soga et al.[7] find a value of 4–5 by ^{13}C NMR. For $TiCl_4/Mg$ (n-C_6) the $\overline{r_1r_2}$ value from eq 2 is 0.39,[14] and from our ^{13}C NMR measurements it is 1.10 (Table VIII). Thus large differences exist between r_1r_2 values calculated by the two different methods. We feel that the data correlation provided by the copolymerization equation for multiple-species catalysts is fortuitous, and although it provides a useful tool for predicting polymer composition, fundamental significance is lacking.

If a sequence distribution is adequately represented by a multiple-species model, the $\overline{r_1r_2}$ value from eq 1 will obviously depend in some way on the r_1 and r_2 of the individual species. Cozewith and Ver Strate[12] calculated that for a two-species catalyst $\overline{r_1r_2}$ lies between the species r_1r_2 values for r_1 and r_2 typical of soluble vanadium catalysts. If r_1r_2 for each species is 1, Ross[9] shows that $\overline{r_1r_2}$ is always greater than 1. We have further explored the dependence of $\overline{r_1r_2}$ on $(r_1)_i$ and $(r_2)_i$ by calculating the averages for a two-species catalyst over a range of conditions. The calculations indicate that if the r_1r_2 values are equal for each species, $\overline{r_1r_2}$ always exceeds this value and increases as the composition difference between the two polymer fractions increases. If $(r_1r_2)_1$ is not equal to $(r_1r_2)_2$, $\overline{r_1r_2}$ also depends on the composition difference between the two copolymers and may be higher or lower than the larger of the two r_1r_2 values.

As illustrated by the plot of $\overline{r_1r_2}$ vs. f_1 in Figures 4 and 5 for the two sets of reactivity ratios that follow:

	case 1			case 2		
	r_1	r_2	r_1r_2	r_1	r_2	r_1r_2
species 1	5	0.05	0.25	5	0.8	4
species 2	40	0.1	4	40	0.006 25	0.25

$\overline{r_1r_2}$ lies between the component reactivity ratio products if the $(r_1)_i$ and $(r_2)_i$ values are such that the composition difference between copolymer fractions is not very large (Figure 4). However, for large differences in composition,

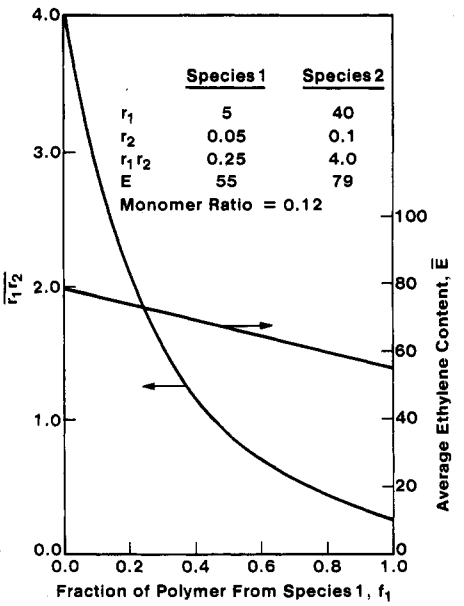

Figure 4. Dependence of $\overline{r_1r_2}$ on f_1 for small compositional difference.

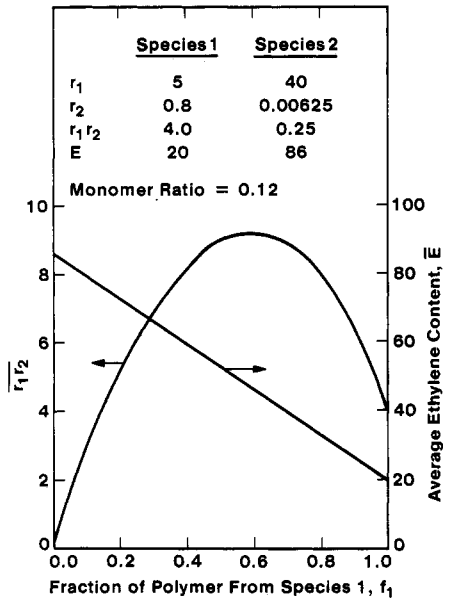

Figure 5. Dependence of $\overline{r_1r_2}$ on f_1 for large compositional difference.

$\overline{r_1r_2}$ exceeds the component reactivity ratio products (Figure 5). Although calculations have only been made for a two-species catalyst, we believe r_1r_2 will behave similarly if more than two species are present. In view of the complex dependence of $\overline{r_1r_2}$ on the individual reactivity ratios, little can be concluded about the nature of the catalyst species from the determination of $\overline{r_1r_2}$ alone.

To test the suitability of ^{13}C NMR data for determining polymer heterogeneity, the triad and diad concentrations that would actually be present in a two-component polymer blend with r_1r_2 equal to 1 for each component was calculated for several component fractions (f_1) and compositions (E_1, E_2). The average polymer composition was held constant at 50 mol % ethylene. These calculated values were then fit by the single-species model to obtain $\overline{r_1r_2}$ and predicted sequence concentrations. As shown by the case A results in Table X, the sum of the squares for a 50/50 blend of a 60 and 40 mol % copolymer would meet our criteria for a good fit to the model, and this polymer would appear to have been made by a single catalyst

Table X
Effect of Copolymer Fraction Composition on Average Sequence Concentration

		case					
		A		B		C	
	$\bar{E}$, mol %	50		50		50	
	f_1	0.50		0.50		0.80	
	E_1, mol %	60		20		42.5	
	E_2, mol %	40		80		80	
	$\overline{r_1r_2}$	1.18[a]		5.64[a]		1.45[a]	
	calcd[b]	predicted[a]	calcd[b]	predicted[a]	calcd[b]	predicted[a]	
PP	0.26	0.26	0.34	0.35	0.27	0.27	
EP	0.48	0.48	0.32	0.30	0.45	0.45	
EE	0.26	0.26	0.34	0.35	0.27	0.27	
PPP	0.14	0.14	0.26	0.25	0.16	0.15	
PPE	0.24	0.25	0.16	0.21	0.22	0.25	
EPE	0.12	0.11	0.08	0.044	0.12	0.10	
PEP	0.12	0.11	0.08	0.044	0.11	0.10	
EEP	0.24	0.25	0.16	0.21	0.24	0.25	
EEE	0.14	0.14	0.26	0.25	0.15	0.15	
10^{-4}SS[c]		2.8		8.4		15	

[a] Best fit values from least-squares, single species model. [b] Calculated from fraction compositions. [c] Sum of squares of deviations.

species. However, a 50/50 blend of an 80 and 20 mol % copolymer (case B) gives a large sum of the squares value and $\overline{r_1r_2}$ is much higher than the r_1r_2 of 1 for the components. We could readily establish the heterogeneity of this copolymer by ^{13}C NMR. Case C in the table represents the situation where 20% of a high-ethylene-content copolymer is mixed with a copolymer of moderate ethylene content. $\overline{r_1r_2}$ is 1.45, and the heterogeneity of this copolymer could also be distinguished by ^{13}C NMR.

Conclusions

^{13}C NMR measurement of the diad and triad distribution in ethylene–propylene copolymers is a very useful technique for polymer characterization. This data is even more valuable if it can be used to determine reactivity ratios that allow calculation of the entire monomer sequence distribution or yield information about the nature of the catalyst. In this paper we have shown that for ideal copolymers, made by a single catalyst species at constant monomer concentration, experimental diad and triad data are well correlated by the equations derived from copolymerization theory and consequently the reactivity ratios determined from these equations should be reliable indicators of sequence distribution. The accuracy of the predictions, as measured by the sum of the squares of the deviations, provides a yardstick for deciding whether the diad and triad concentrations for a particular sample are consistent with a single-species catalyst. However, we have also shown that blends of polymers with compositions differing by as much as 20 mol % ethylene can give an excellent fit to the single-species model. Thus ^{13}C NMR is not a sensitive technique for unequivocally establishing the presence of only one species, and additional confirmation by MWD or polymer compositional distribution measurement is highly desirable.

When multiple-catalyst species exist, ^{13}C NMR diad and triad distributions provide enough information to test whether all of the species have $(r_1r_2)_i$ equal to 1, and if so, whether there are two or more than two species present. If there are exactly two species, the amount and composition of the two polymers produced can be determined. Analysis of ^{13}C NMR data for EPM copolymers produced by a variety of heterogeneous titanium catalysts indicated that multiple catalyst species were present in all cases, and for several catalysts the two species, $r_1r_2 = 1$ model seemed appropriate. However, in general, the compositional distribution of these copolymers appears quite broad, indicating the presence of more than two catalyst species, and the r_1r_2 for the individual species is estimated to lie in the range of at least 0.5 to 3.0. For polymers of this complexity, ^{13}C NMR data alone is of little use in providing detailed information about the nature of the catalyst. For multiple-species catalysts, $\overline{r_1r_2}$ determined by a least-squares fit of diad and triad data to the single-catalyst-species equations is relatively independent of composition but is more a function of compositional distribution than monomer sequence distribution.

We also show in this paper that the average $\overline{r_1r_2}$ for heterogeneous titanium catalysts determined by fitting polymer composition/monomer concentration data to the copolymerization equation is much lower than the value obtained from the diad distribution and eq 1. As a result, $\overline{r_1r_2}$ values determined from the copolymerization equation cannot be used to conclude anything about sequence distribution.

Acknowledgment. We are grateful to Dr. E. Tornqvist for supplying some of the polymers examined, Dr. D. M. Cheng for the ^{13}C NMR spectra, and Dr. S. Floyd for helpful discussions of part of this work.

Registry No. EPM, 9010-79-1; E, 74-85-1; P, 115-07-1; Ti, 7440-32-6; Al, 7429-90-5.

References and Notes

(1) Wilkes, C. E.; Carmen, C. J.; Harrington, R. A. *J. Polym. Sci.* **1973**, *43*, 237–250.
(2) Ray, G. J.; Johnson, P. E.; Knox, J. R. *Macromolecules* **1977**, *10*, 773–778.
(3) Randall, J. C. *Macromolecules* **1978**, *11*, 33–36.
(4) Cheng, H. N. *Macromolecules* **1984**, *17*, 1950–1955.
(5) Kakugo, M.; Naito, Y.; Mizunuma, K.; Mujatake, T. *Macromolecules* **1982**, *15*, 1150–1152.
(6) Doi, Y.; Ohnishi, R.; Soga, K. *Makromol. Chem., Rapid Commun.* **1983**, *4*, 169–174.
(7) Soga, K.; Shiono, T.; Doi, Y. *Polym. Bull (Berlin)* **1983**, *10*, 168–174.
(8) Cheng, H. N. *Anal. Chem.* **1982**, *54*, 1828–1833.
(9) Ross, J. F. *J. Macromol. Sci., Chem.* **1984**, *A21*(4), 453–472.
(10) Ross, J. F. International Symposium on Transition Metal Catalyzed Polymerization, Akron, OH, June 16, 1986, paper 60.
(11) Randall, J. C. *Polymer Sequence Determination*; Academic: New York, 1977.
(12) Cozewith, C.; Ver Strate, G. *Macromolecules* **1971**, *4*, 482–489.
(13) Kashiwa, N.; Mizuno, A.; Minami, S. *Polym. Bull (Berlin)* **1984**, *12*, 105–109.
(14) Soga, K.; Ohtake, M.; Ohnishi, R.; Doi, Y. *Polym. Commun.* **1984**, *25*, 171–173.